6. A. Taragin. Effect of Roadway Width on Traffic Operations--Two Lane Concrete Roads. Proc., HRB, National Research Council, Washington, D.C., Vol. 24, 1944, pp. 292-318.
7. Vehicle Speed and Placement Survey on Two Lane Rural Highways. Road Design Division, Texas Highway Department, Austin, March 1957.
8. D.H. Weir and C.S. Sihilling. Measures of Lateral Placement of Passenger Cars and Other Vehicles in Proximity to Inner City Buses on Two Lane and Multi-Lane Highways. Final Report. Environmental Design and Control Division, FHWA, U.S. Department of Transportation, Oct. 1972.
9. E.J. Miller and G.N. Stuart. Vehicle Lateral Placement on Urban Roads. Journal of the Transportation Engineering Division, ASCE, Vol. 108, Sept. 1982.
10. E. Ellard. Vehicle Size-Lane Width Interaction: A Pilot Project. M.S. thesis. University of Toronto, Toronto, Canada, 1975.
11. P.R. Shankar. Lateral Placement of Truck Traffic in Highway Lanes. Ph.D. dissertation. University of Texas at Austin, 1984.
12. J.J. Panak and H. Matlock. A Discrete-Element Method of Analysis for Orthogonal Slab and Girder Bridge Floor Systems. Research Report 26-25. Center for Highway Research, University of Texas at Austin, May 1972.
13. A.S. Vesic and S.K. Saxena. Analysis of Structural Behavior of AASHO Road Test Rigid Pavements. NCHRP Report 97. HRB, National Research Council, Washington, D.C., 1970.

Publication of this paper sponsored by Committee on Rigid Pavements.

ILLI-PAVE Mechanistic Analysis of AASHO Road Test Flexible Pavements

ROBERT P. ELLIOTT and MARSHALL R. THOMPSON

ABSTRACT

The stress-dependent, finite element pavement model known as ILLI-PAVE was used to study the performance of AASHO Road Test flexible pavement sections. Analyses were conducted to identify significant relationships between the appearance of fatigue cracking in the asphalt concrete (AC) surface and the AC strain and subgrade deviator stress predicted by ILLI-PAVE. Deflection and temperature data from the road test were used with ILLI-PAVE to "back calculate" seasonal variations in subgrade support and load-induced pavement stresses and strains. The structural response-performance relationships identified explain the observed behavior of the AASHO Road Test pavement sections in a realistic fashion. Seasonal damage factors and weighting factors based on these relationships provide a mechanistic explanation of the seasonal effects that is consistent with experience. These results demonstrate that ILLI-PAVE is a powerful tool for pavement design and analysis. It provides an adequate and valid representation of the structural behavior of conventional flexible pavements and can be used to effectively evaluate nondestructive test (NDT) data and determine the structural characteristics of existing pavement systems. ILLI-PAVE, therefore, will serve as a sound basis for the development of mechanistic procedures for the design of new flexible pavements and for the selection of rehabilitation strategies for existing flexible pavements.

In a preliminary effort to select transfer functions for a mechanistic flexible pavement design procedure, the performance of the flexible pavement sections of Lane 1, Loop 4 of the AASHO Road Test was studied. The mechanistic design procedure is to be based on the structural response predictions (stresses, strains, and deflections) of the stress-dependent, finite element pavement model known as ILLI-PAVE. This model was selected on the basis of previous studies by Figueroa (1) and Hoffman and Thompson (2) that showed that ILLI-PAVE provided reliable and realistic predictions of the structural behavior of pavement. Simplified equations, referred to as ILLI-PAVE structural response algorithms, were developed (3) that predict the "critical" response parameters for the standard 18-kip single axle load. The AASHO Loop 4 pavement sections selected for study had been subjected to 18-kip single axle loads and thus were compatible with the stresses and strains predicted by the ILLI-PAVE algorithms.

In mechanistic pavement design, the pavement system is analyzed on the basis of the predicted structural response (stresses, strains, and deflections) of the system to moving vehicle loads. Pavement layer thicknesses (surface, base, and subbase) are selected to resist the detrimental effects of these predicted response parameters for some desired number of load repetitions. The relationships used for thickness selection are collectively referred to as transfer functions. Transfer functions relate structural response to pavement performance. However, because the predicted stresses, strains, and deformations for a given pavement are not the same for all structural models, the transfer functions are "model dependent" and must be developed for the model used in the design procedure.

The AASHO Road Test pavements were studied to identify significant relationships between the appearance of fatigue cracking in the AC surface and the AC strain and subgrade deviator stress predicted by the ILLI-PAVE structural response algorithms. Flexible pavement cracking at the road test was divided into three classes. The first to appear were fine, disconnected hairline cracks called Class 1. As these lengthened, widened, and connected to form an alligator crack pattern, they were classified as Class 2 cracks. The cracking was called Class 3 when the crack edges became spalled and the individual pieces loosened and moved under traffic. The analyses discussed here were based on the appearance of Class 1 cracks.

MATERIAL CHARACTERIZATION

ILLI-PAVE includes stress-strain material characterization models that realistically represent the nonlinear, stress-dependent resilient behavior of granular materials and fine-grained soils. Included in the model is a shear strength-based "stress adjustment" feature that compensates for predicted stresses that exceed the actual strength of the granular base and subgrade materials (e.g., tensile stresses in the granular base). This feature has been described by Raad and Figueroa (4).

The basic relationship used to model the behavior of granular base material is

$$Er = K\theta^n \tag{1}$$

where

Er = resilient modulus of the material;
K,n = constants determined from laboratory testing; and
θ = the sum of the three principal stresses, $\sigma_1 + \sigma_2 + \sigma_3$ (in triaxial testing $\theta = \sigma_1 + 2\sigma_3$).

The ILLI-PAVE algorithms were developed (3) using K and n values for the AASHO Road Test granular materials reported by Traylor (5).

The behavior of fine-grained subgrade soil is represented by two intersecting, arithmetic, straight line relationships as shown in Figure 1. The mathematical expression for the model is

$$Er = Eri + K1 \cdot (Sd - Sdi) \qquad \text{for } Sd < Sdi \tag{2}$$

and

$$Er = Eri + K2 \cdot (Sd - Sdi) \qquad \text{for } Sd > Sdi \tag{3}$$

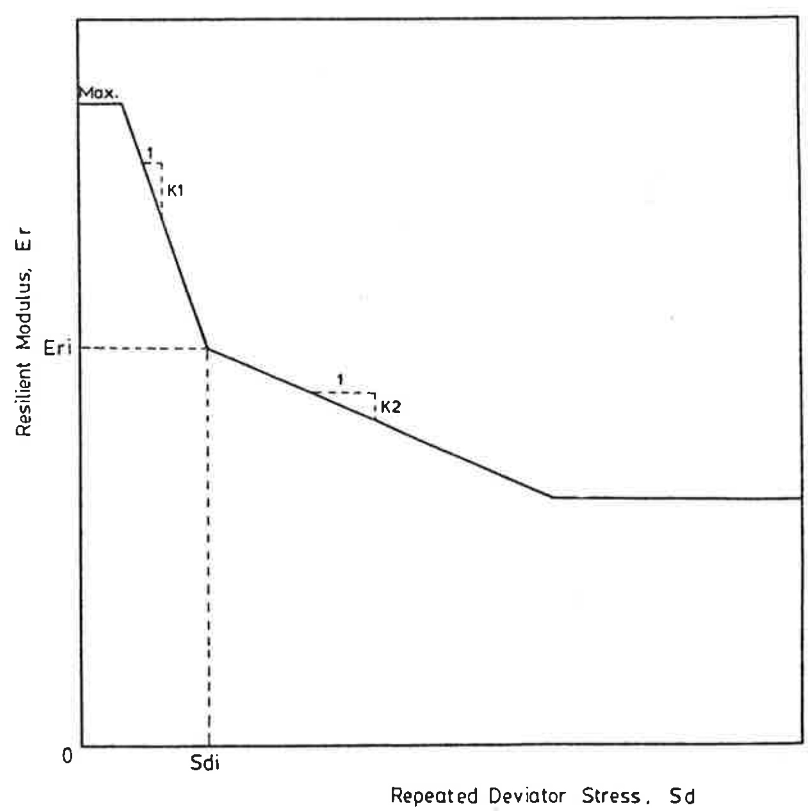

FIGURE 1 Typical representation of the resilient modulus-repeated deviator stress relationship for fine-grained soils.

where

Er = resilient modulus,
Eri = resilient modulus at the "breakpoint" between the two Er versus Sd slopes,
K1,K2 = slopes of the Er versus Sd relationship,
Sd = deviator stress, and
Sdi = deviator stress at the breakpoint between the ER versus Sd slopes.

The K1, K2, and Sdi values used in developing the ILLI-PAVE algorithms were based on the results of an extensive study of Illinois soils (including the AASHO subgrade) by Thompson and Robnett (6).

Asphalt concrete (AC) is modeled in ILLI-PAVE as a linear elastic solid. For this study, the AC modulus (Eac) was calculated using the equation developed by the Asphalt Institute (7) with mix data reported from the road test (8). Figure 2 shows a plot of the temperature-Eac relationship used in the analyses. For comparison, laboratory test results on AC samples taken from the road test pavements and reported by Austin Research Engineers (9) are shown.

ANALYSIS OF SUBGRADE VARIATION

Two types of algorithms were used in the study, design response algorithms and pavement analysis algorithms. The design response algorithms predict the critical stress and strain in the pavement system due to an 18-kip single axle load. The prediction is made on the basis of the AC thickness, the granular base thickness, the AC modulus, and the subgrade Eri. The design response algorithms will serve as the basis of the mechanistic design procedure.

The pavement analysis algorithms are for use in analyzing the structural response of existing pavements using nondestructive testing (NDT) data. The NDT data are used to "back calculate" subgrade Eri and to estimate the load-induced stresses and strains.

For this study, the pavement analysis algorithms were used to determine the apparent seasonal variation in the subgrade Eri during the road test. The Benkelman beam deflection data from the road test were converted to equivalent moving wheel load deflections by multiplying the deflection measurements by 0.62. This conversion was based on speed-deflection studies conducted during the road test (8). AC modulus variation was estimated using the average AC temperature reported at the time of deflection testing (Figure 3). These Eac values and the deflections of each pavement section were used in the analysis algorithms to estimate subgrade Eri's at the time of testing. Only sections that had not yet cracked at the time of testing were included in the analyses of each period. The average Eri for all sections analyzed was selected as the Eri for each deflection test date. Figure 4 shows a plot of seasonal vari-

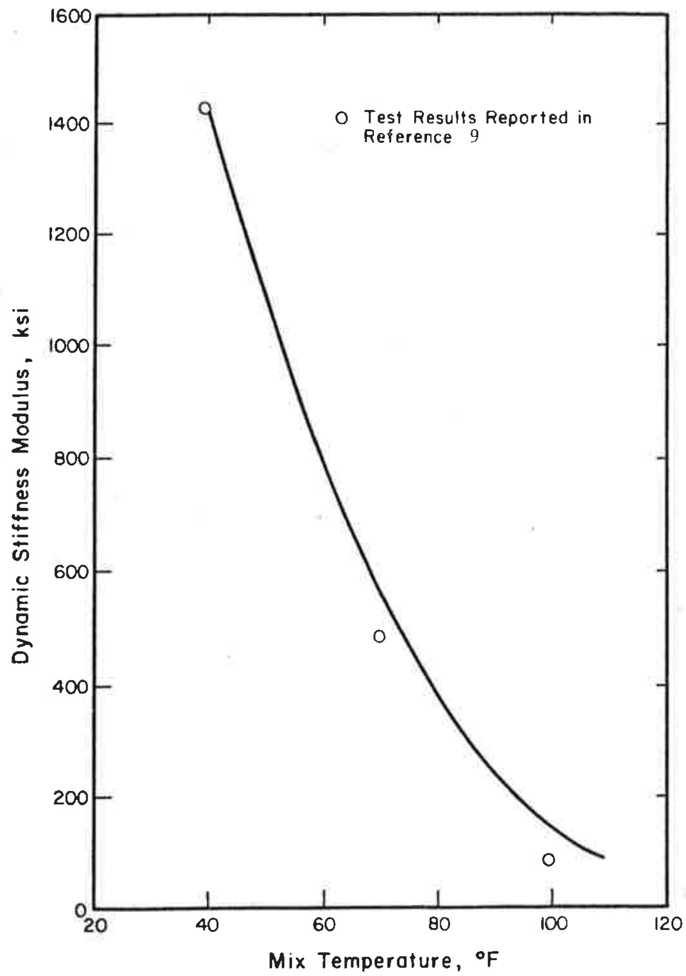

FIGURE 2 AC mix temperature-modulus relationship used in analysis of AASHO Road Test sections.

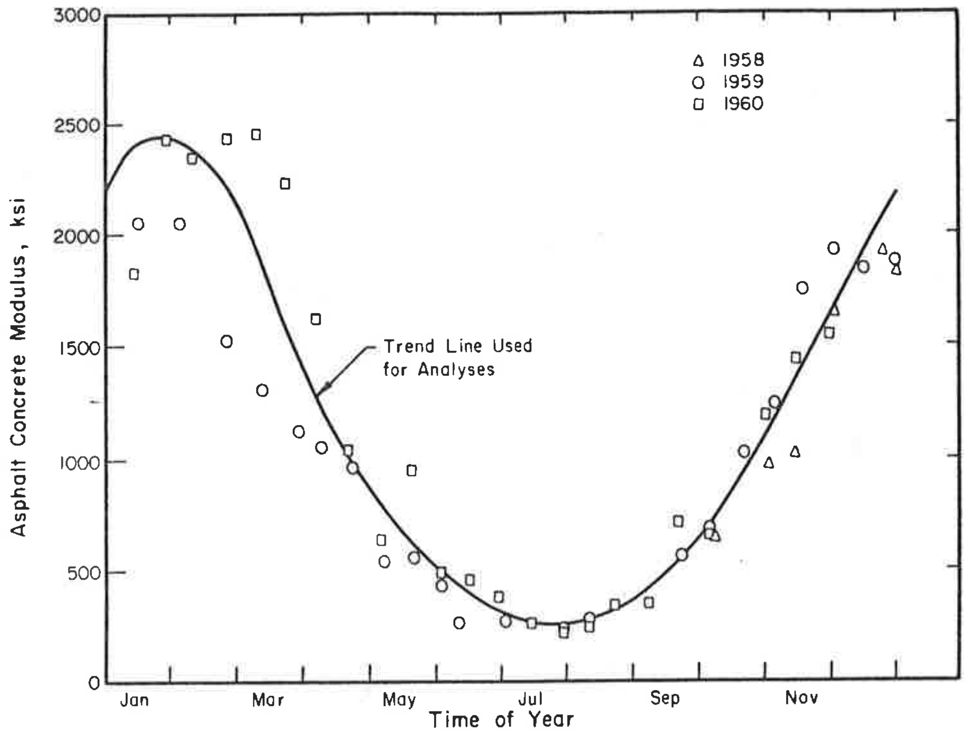

FIGURE 3 Trend of AC modulus during AASHO Road Test.

ation in subgrade Eri. The Eac and Eri trends shown in Figures 3 and 4 were subsequently used with the design response algorithms for the structural response-performance analyses.

EFFECT OF GRANULAR TYPE ON STRUCTURAL RESPONSE

ILLI-PAVE model analyses based on K and n values typical of crushed stone and gravel base courses showed that the type of granular material has only a limited effect on the structural response (stresses, strains, and deflections) of the pavement system (3). For design purposes, the response differences were not deemed sufficient to warrant including granular type as a variable in the ILLI-PAVE algorithms. Therefore only base thickness, with no differentiation for material type, was included.

Deflection data from the AASHO Road Test were analyzed to determine the validity of this decision. Both gravel and crushed stone were used in the road test flexible pavements. The crushed stone was referred to as the base course and the gravel was called the subbase. In Loop 4, base course thicknesses were 0, 3, and 6 in. Subbase thicknesses were 4, 8, and 12 in. Each possible combination of these thicknesses was used with AC thicknesses of 3, 4, and 5 in. Deflection data gathered during the early phases of the test (before significant damage was done to any of the pavements) were analyzed to determine the relative effect of each type of granular material on structural response. For the 3-in. AC sections, data from the first two measurement periods were used. Data from the first three periods were used for the 4- and 5-in. thicknesses.

Correlation and regression analyses were conducted using the measured deflections as the dependent variable and the thickness of granular material as the independent variable. Two types of analyses were made, one using the total, combined granular thickness (crushed stone plus gravel) as a single independent variable and the other using the two thicknesses as separate independent variables. The data for each AC thickness were analyzed individually to eliminate any thickness interaction effect.

Comparison of the correlation coefficients and standard errors of estimate for the two types of analysis were used as an indication of the relative significance of separating or combining the thicknesses in terms of structural response. Table 1 gives the results of the analyses. In general, the correlation coefficients were slightly higher when the separate thicknesses were used; however, standard errors of estimate were nearly the same for both cases with an equal split between the separate and combined thickness analyses in the number that produced the lower standard error of estimate (four each). These results demonstrate that the type of granular material has little effect on structural response of pavement.

This should not be interpreted to imply that the type and quality of granular material do not influence pavement performance. The structural re-

TABLE 1 Analysis of Early AASHO Road Test Data for the Relative Effects of Granular Base and Subbase

Section Asphalt Thickness (in.)	Testing Index Day	Correlation Coefficient		Standard Error of Estimate	
		Separate[a]	Combined[b]	Separate[a]	Combined[b]
3	827	0.84	0.81	14.5	14.4
3	871	0.80	0.79	16.6	16.0
4	827	0.91	0.83	6.3	8.0
4	871	0.89	0.71	4.1	6.0
4	997	0.87	0.64	11.3	16.6
5	827	0.78	0.78	7.9	7.4
5	871	0.79	0.72	5.9	6.2
5	997	0.83	0.83	6.1	5.7

[a]The thickness of base and subbase were treated as two independent variables.
[b]Base and subbase thicknesses were added and treated as a single independent variable.

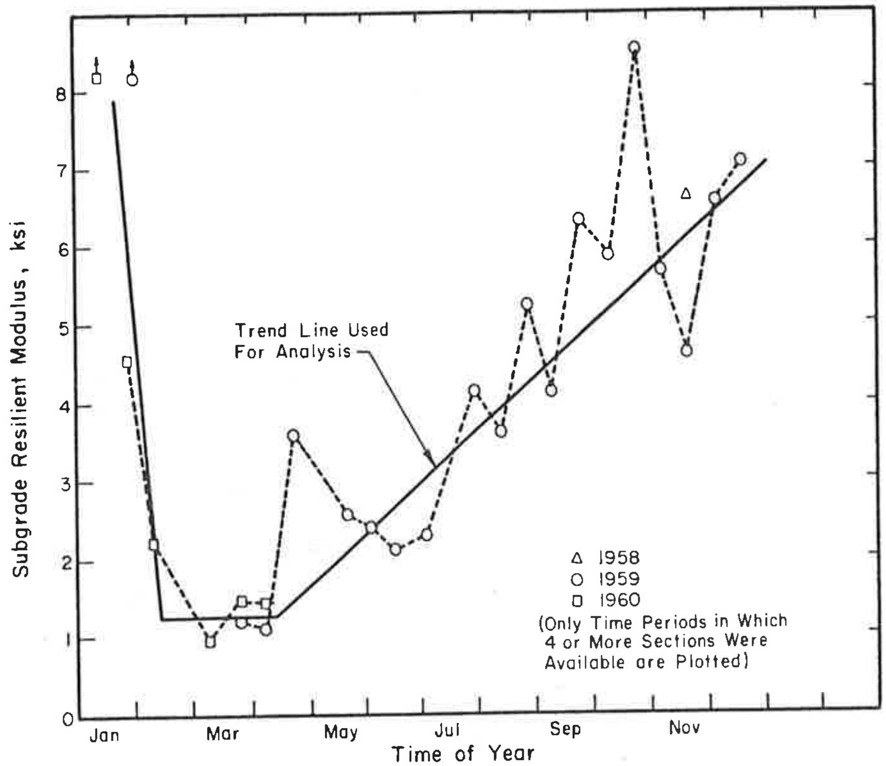

FIGURE 4 Trend of subgrade Eri during AASHO Road Test.

sponse may be similar but the relationships between response and performance will differ. Differing design criteria related to performance (or differing transfer functions) must be established for various types and qualities of base.

ASPHALT STRAIN VERSUS CRACKING

Fatigue Relationships for Asphalt Concrete

Except for temperature cracks and long-term weathering cracks, AC surface cracking in conventional flexible pavements is normally considered to be associated with fatigue. Thus there should be some relationship between the radial strain at the bottom of the AC layer and the number of load repetitions to crack appearance. Laboratory testing indicates that the relationship can be expressed in the form:

$$N = K \cdot eac^a \tag{4}$$

where

N = number of load repetitions to cracking,
K = multiplication constant determined by testing,
eac = magnitude of load-induced strain, and
a = power constant determined by testing.

Laboratory testing is conducted under controlled conditions in which the temperature of the mix does not vary and either the applied stress or the induced strain is held constant. In actual pavements each of these items changes continuously over the life of the pavement, complicating the behavioral relationships. For the AASHO pavements, this is somewhat simplified because the loading was constant. However, with the seasonal variations in subgrade support conditions and the changes in AC modulus due to temperature fluctuations, the AC strain variations over the life of the pavements are quite large and complicated.

Research reported by Bonnaure et al. (10) and by Finn et al. (11) indicate that the fatigue effect of the load-induced strain is a function not only of the strain magnitude but also of the modulus of the AC. This has been expressed as fatigue equations having the general form:

$$N = K \cdot eac^a \cdot Eac^b \tag{5}$$

where Eac is the AC dynamic stiffness modulus and b is a power constant determined by testing.

Equation 5 quantifies some of the AC temperature variation effects but does not address the problems associated with variations in the strain value itself. To account for the strain variations, Miner's hypothesis of damage accumulation has been used with reasonable success with numerous materials including AC (12). This hypothesis together with the general fatigue equation shown previously was employed in analyzing the road test pavements.

Miner's hypothesis can be expressed mathematically in terms of relative damage factors. Cracking is expected to occur when the sum of the damage factors equals one. The equation for the damage factors is

$$Di = ni/Ni \tag{6}$$

where

Di = relative damage during some period i,
ni = number of load applications during the period, and
Ni = total number of load applications the pavement could carry for the strain induced under the conditions prevailing during the period.

In Equation 6 Ni is determined by a fatigue equation of the form shown previously and is a function of the load-induced strain (eac) and AC modulus. The object of the analyses was to select appropriate values for the fatigue equation constants K, a, and b. The approach taken in the analyses was to (a) select reasonable estimates of the appropriate values for a and b, (b) use these values with the road test data and the design algorithm for AC strain to calculate average Ks for each combination of a and b for all sections, and (c) select the K, a, and b combination that provides the best prediction of the actual data.

Selection of a and b Values for Fatigue Analysis

Three tentative values were selected for b. These were -0.854, -1.4, and -1.8. The first value was selected on the basis of Finn's analysis (12) of the fatigue behavior of the road test pavements. The other two values were taken from the fatigue equations reported by Bonnaure et al. (10).

Preliminary estimates of the a constant were made using the deflection-based performance equations from the AASHO Road Test (8) with the deflection algorithm developed in another study (3). Two performance-deflection equations were available from the road test. One was for the number of load applications to a present serviceability index of 2.5 (the point at which most major highways are rehabilitated); the other was to a present serviceability index of 1.5 (the point at which the road test pavements were removed from test). The equations are

$$\log N2.5 = 9.40 + 1.32 \cdot \log L - 3.25 \cdot \log dsn \tag{7}$$

and

$$\log N1.5 = 10.18 + 1.36 \cdot \log L - 3.64 \cdot \log dsn \tag{8}$$

where

N2.5 and N1.5 = number of axle load applications to a present serviceability index of 2.5 and 1.5, respectively;
L = axle load in kips; and
dsn = spring normal Benkelman beam deflection.

As discussed previously, Benkelman beam deflections from the road test were converted for purposes of analysis to equivalent dynamic deflections by multiplying by 0.62. Substituting this conversion and the standard 18,000-lb (18-kip) axle load value into Equations 7 and 8 yields

$$\log N2.5 = 10.3822 - 3.25 \cdot \log Do \tag{9}$$

and

$$\log N1.5 = 11.1315 - 3.64 \cdot \log Do \tag{10}$$

where Do is the dynamic surface deflection in mils.

One algorithm has been developed (3) to estimate AC strain (eac) based on surface deflection. This algorithm is

$$\log eac = -5.0898 + 1.1126 \cdot \log Do \qquad SEE = 0.115 \qquad R^2 = 0.79 \tag{11}$$

where eac is tensile strain in the bottom of the AC, in inches per inch. Solving for log Do and substituting this into Equations 9 and 10, performance equations in the form of AC fatigue equations are obtained. These equations are

$$\log N2.5 = -4.4856 - 2.92 \cdot \log eac \tag{12}$$

and

$$\log N1.5 = -5.5204 - 3.27 \cdot \log eac \tag{13}$$

The constants 2.92 and 3.27 are analogous to the a constant of the fatigue equation. These values were taken as an approximation of the value for a that would best represent the fatigue properties of the AASHO Road Test mixes.

Two values for a in this general range were subsequently selected for use in the analyses. These were 3.16 and 3.29. The 3.16 value was taken from work reported by Thompson (13), and the 3.29 value came from the fatigue equation developed by the Asphalt Institute (7) in their analysis of the AASHO Road Test.

Determination of K Coefficient

A computer analysis program was developed for determining fatigue equation K coefficients. The program analyzed each AASHO pavement section from Lane 1 Loop 4 using all combinations of the a and b values selected. The program was based on Miner's hypothesis of accumulated damage and used the AC strain design algorithm. Algorithm inputs were the material thicknesses of each section and AC modulus and subgrade Eri's for each analysis period.

For purposes of analysis, the total time of the road test was divided into as many discrete periods as possible. The number of periods and their length were dictated by the time between deflection testing during the road test. In general, 2-week periods were used. The controlling factor was the date on which surface deflections were measured and reported because these data were used to estimate the subgrade Eri. Each analysis period then was the time between successive dates of deflection measurement.

AC modulus values for each analysis period were determined using the Asphalt Institute equation and the average measured AC temperature during the period. Eri values were selected on the basis of the work discussed under "Analysis of Subgrade Variation." For analysis periods from the start of the road test until late in the second spring, the average of the section Eri values was selected as the best estimate of the day of test Eri; and the average of two consecutive days of test Eri's was selected as the subgrade Eri for the analysis period. By late in the second spring, only four analysis sections remained that had not developed cracking. This number was not considered sufficient to provide a good Eri estimate. For the remainder of the analysis periods, Eri values were selected on the basis of the seasonal trend of values established from the earlier periods.

Table 2 gives the end dates of the analysis periods, the modulus values used for each period, and the total number of 18-kip single axle loads applied to the road test pavements to the end of the period.

The analysis program calculated damage factors (Di) for each pavement section during each analysis period using the number of axle applications during the period (ni) and the fatigue equation (Ni) with the K coefficient set equal to 1.0. For those periods in which the Eri is listed as "frozen," the damage factor was set equal to zero. Each section's damage factors were accumulated until the total number of axle applications equaled that reported for the occurrence of cracking.

With the K coefficient set equal to 1.0, each section's damage factor sum provided an estimate of

TABLE 2 Material and Load Application Data Used in Analysis of AASHO Road Test Pavement Sections

Period End Date	Total Axle Loads	Eac (ksi)	Eri (ksi)	Period End Date	Total Axle Loads	Eac (ksi)	Eri (ksi)
10/7/58	400	622	5.0	12/16/59	375,440	1,818	6.8
11/3/58	1,280	964	5.4	12/30/59	385,800	1,860	7.0
11/14/58	3,760	1,000	5.9	12/30/59	385,800	1,860	7.0
12/3/58	11,620	1,607	6.3	1/13/60	407,960	1,818	Frozen
12/24/58	25,460	1,900	6.7	1/27/60	445,200	2,423	Frozen
12/31/58	28,920	1,800	7.0	2/10/60	480,940	2,348	3.4
1/14/59	35,660	2,059	Frozen	2/24/60	507,280	2,423	1.9
2/4/59	52,300	2,060	Frozen	3/9/60	542,380	2,459	1.3
2/25/59	69,920	1,508	Frozen	3/23/60	572,360	2,230	1.2
3/11/59	75,780	1,300	1.2	4/6/60	603,460	1,610	1.3
3/27/59	79,600	1,116	1.2	4/20/60	636,040	1,037	1.3
4/8/59	86,120	1,054	1.1	5/4/60	671,200	624	1.6
4/22/59	97,580	964	2.3	5/18/60	707,180	938	1.9
5/6/59	106,620	535	3.3	6/1/60	735,100	488	2.2
5/20/59	119,360	556	2.8	6/15/60	774,440	448	2.5
6/3/59	136,220	420	2.5	6/29/60	809,760	392	2.8
6/10/59	143,660	250	2.3	7/13/60	836,320	257	3.1
7/1/59	169,140	262	2.3	7/27/60	871,400	211	3.5
7/29/59	201,120	225	3.2	8/10/60	905,780	222	3.8
8/12/59	219,040	275	3.9	8/24/60	932,040	327	4.1
9/9/59	251,920	312	4.3	9/7/60	953,860	327	4.4
9/23/59	273,900	553	5.2	9/21/60	988,480	701	4.7
10/5/59	292,480	675	6.1	10/5/60	1,213,360	649	5.0
10/21/59	306,042	1,004	7.2	11/2/60	1,085,900	1,179	5.4
11/4/59	324,720	1,216	7.1	11/16/60	1,103,840	1,408	5.9
11/18/59	338,160	1,734	5.2	11/30/60	1,113,760	1,528	6.3
12/2/59	354,400	1,901	5.6				

the K coefficient appropriate to that section and combination of a and b coefficients. That is, if that value were used for K, the sum of the damage factors for the section would be 1.0. The average of the damage factor sums for all sections for each a and b combination was selected as the best overall estimate of the K coefficient.

Damage factor sums for each a and b combination were subsequently determined for all sections using these K coefficients. The means and standard deviations of the damage factor sums were then calculated. The means, of course, were all 1.0 because of the method used to select K. The variation in the standard deviations was relatively small, ranging from 1.05 to 1.09. The a and b combination producing the lowest standard deviation was selected. The resulting equation is

$$\log N = 2.2340 - 3.16 \cdot \log eac - 1.4 \cdot \log Eac$$

$$SEE = 0.40 \qquad R^2 = 0.53 \tag{14}$$

where

N = predicted number of 18,000-lb axle load applications to crack appearance;
eac = predicted AC strain, in inches per inch; and
Eac = dynamic stiffness modulus of the AC, in psi.

A plot of the actual versus predicted numbers of load applications using this equation is shown in Figure 5.

SUBGRADE DEVIATOR STRESS VERSUS LOAD APPLICATIONS

It is generally recognized, and the Road Test results confirm, that spring is the most critical time of year in terms of distress development in conventional flexible pavements. In recognition of this, the relationship between crack development and subgrade deviator stress was studied in terms of the predicted stress for typical spring conditions at the road test.

A subgrade deviator stress for each pavement section was predicted for typical spring conditions. The modulus values used to represent spring conditions (Eac = 1,340 ksi and Eri = 1.4 ksi) were selected on the basis of an analysis of seasonal load damage effects (3).

The predicted stresses were then related to the number of 18-kip single axle loads applied to each section before Class 1 cracking was observed. This produced the following equation:

$$\log N = 7.2558 - 0.6378 \cdot sd \qquad SEE = 0.23 \qquad R^2 = 0.82 \tag{15}$$

where

N = number of 18-kip single axle applications and
sd = predicted subgrade deviator stress.

The correlation coefficient for this equation is 0.908; and the standard error of estimate is 0.233. In terms of typical pavement life predictive equations, these two statistical parameters show the equation and relationship to be quite good. Figure 6 shows a plot of the predicted versus actual number of load applications for the analysis sections using this equation.

MODIFIED FATIGUE RELATIONSHIP

For comparison purposes, the 18-kip single axle applications to Class 1 AC cracking were predicted using the subgrade deviator stress relationship (Equation 15) and the AC strain relationship (Equation 14). These two predictions were then compared to the actual numbers of applications. The deviator stress-based prediction was closer to the actual number more frequently than was the AC strain-based prediction. This was particularly true for the thinner pavement sections for which the strain-based prediction was always high. For all sections less than 15 in. in total thickness, the subgrade deviator stress provided the closer prediction.

On the basis of this observation, it was concluded that fatigue was probably not the major cause of cracking in pavements having a total thickness (AC plus granular) of less than 15 in. Cracking in

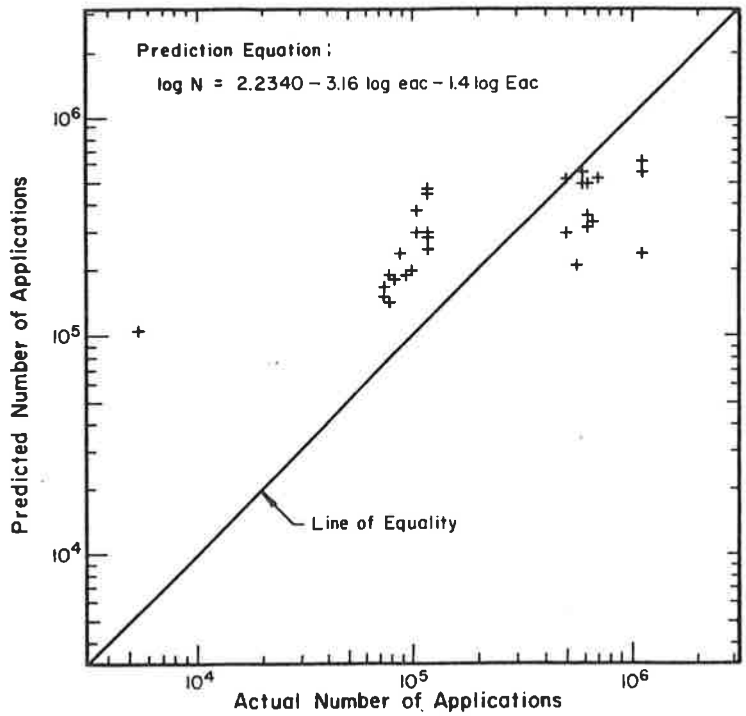

FIGURE 5 Comparison of actual versus predicted 18,000-lb axle applications to Class 1 cracking based on asphalt strain.

these pavements probably was controlled by excess permanent deformation and strain due to overstressing the granular materials and subgrade. Indeed, all of the sections developed significant surface rutting before cracking became apparent, suggesting that permanent deformation and strain (as opposed to the resilient AC radial strain predicted by the algorithms) played a major role in the behavior of all the sections.

To provide a better predictor of fatigue-type crack development, another analysis was conducted using only those sections having a total (AC plus granular) thickness of 15 in. or more. This analysis was conducted in a manner identical to that de-

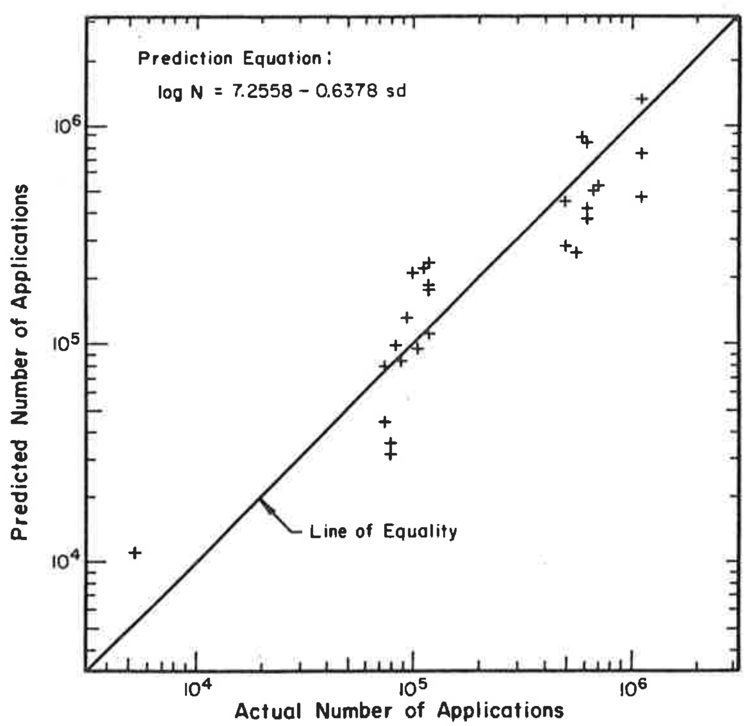

FIGURE 6 Comparison of actual versus predicted 18,000-lb axle applications to Class 1 cracking based on subgrade deviator stress.

scribed under "Determination of K Coefficient." The same a (3.16) and b (1.4) constants were used in the analysis to solve for the K coefficient. The equation produced is

$$\log N = 2.4136 - 3.16 \cdot \log eac - 1.4 \cdot \log Eac$$

$$SEE = 0.30 \qquad R^2 = 0.25 \tag{16}$$

Figure 7 shows a plot of the actual versus predicted number of load applications for the analysis sections using this equation. The modified equation provides a better prediction for the sections that withstood a greater number of load applications before Class 1 cracking was observed.

SEASONAL LOAD-DAMAGE EFFECTS

Equation 16 was used to evaluate the seasonal load-damage effects on the Loop 4 AASHO Road Test flexible pavements. For this analysis, relative damage factors (Di) were determined for each pavement design on a weekly basis using a constant traffic volume. Weekly Eri and AC modulus values were selected from examination of the seasonal trends identified for the road test (Figures 3 and 4). On the basis of frost penetration data from the road test, a 7-week period was selected to represent frozen subgrade conditions. During this time, a 0.0 relative damage factor was assigned. Table 3 gives the weekly AC modulus and Eri values used in the analysis.

The seasonal damage factors are the sum of the weekly factors for each season. In this analysis, the seasons were defined as periods of 13 consecutive weeks with the first week of spring being the first week following the 7 weeks of frozen subgrade. The seasonal periods are given in Table 3.

Results are given in Table 4. Although all AC and base thickness combinations from Loop 4 pavements were examined, only the AC thickness had an effect on the relative seasonal damage factors. Although the total number of load applications (N) increased with thickness of granular material, the relative seasonal effect was the same for any single AC thickness.

Additional analyses were performed for AC thicknesses of from 2 to 6 in. using the weighting factor concept established by Gomez-Achecar and Thompson (14). Under this concept, a weighting factor (WFi) for any time period is determined by the equation

$$WFi = Nf/Nai \tag{17}$$

where

Nf = total number of load repetitions to failure over the pavement's normal life and
Nai = number of load repetitions to failure if the conditions (stiffness moduli) during the period prevailed throughout the life of the pavement.

Weekly weighting factors determined for AC pavement surfacing thicknesses of 2 to 6 in. are shown in Figure 8. The trends displayed in this figure are consistent with the seasonal relationships normally accepted on the basis of pavement performance observation.

For conventional flexible pavements (AC surface on a granular base), spring is generally recognized as the critical time of year in terms of load-induced damage. At the AASHO Road Test, the first observation of cracking was normally reported in the spring and most of the sections taken out of test failed during the spring. The second most severe season is normally considered to be fall, followed by summer. Winter, at least in the northern states, is normally the least severe due to frozen conditions. It is also generally recognized that the relative seasonal severity shifts as the AC thickness increases. Summer is the most critical for full-depth (AC for the entire thickness) pavements. Ac-

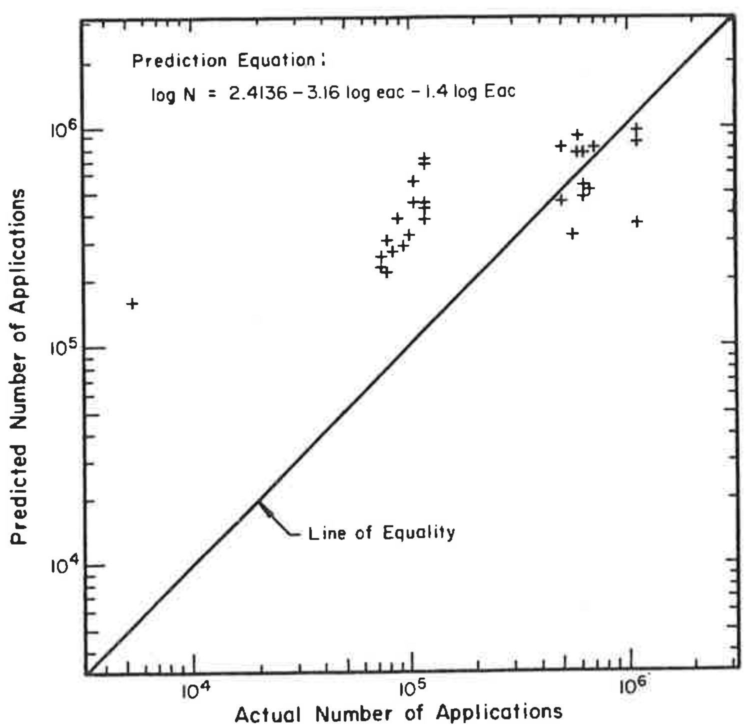

FIGURE 7 Comparison of actual versus predicted 18,000-lb axle applications to Class 1 cracking based on modified AC strain equation.

TABLE 3 Weekly AC Modulus and Subgrade Eri Values Used in Relative Seasonal Effect Analysis

Midweek Date	Asphalt Eac (ksi)	Subgrade Eri (ksi)	Season	Midweek Date	Asphalt Eac (ksi)	Subgrade Eri (ksi)	Season
1/3	2,250	Frozen	Winter	7/4	290	3.1	Summer
1/10	2,380	Frozen	Winter	7/11	260	3.2	Summer
1/17	2,420	Frozen	Winter	7/18	250	3.4	Summer
1/24	2,450	Frozen	Winter	7/25	240	3.6	Summer
1/31	2,430	Frozen	Winter	8/1	250	3.7	Summer
2/7	2,400	Frozen	Winter	8/8	270	3.9	Summer
2/14	2,350	Frozen	Winter	8/15	290	4.0	Summer
2/21	2,280	1.2	Spring	8/22	310	4.2	Fall
2/28	2,240	1.2	Spring	8/29	350	4.3	Fall
3/7	1,950	1.2	Spring	9/5	390	4.5	Fall
3/14	1,770	1.2	Spring	9/12	430	4.6	Fall
3/21	1,600	1.2	Spring	9/19	500	4.8	Fall
3/28	1,440	1.2	Spring	9/26	580	5.0	Fall
4/4	1,300	1.2	Spring	10/3	660	5.1	Fall
4/11	1,150	1.2	Spring	10/10	750	5.3	Fall
4/18	1,040	1.4	Spring	10/17	850	5.4	Fall
4/25	910	1.5	Spring	10/24	970	5.6	Fall
5/2	810	1.7	Spring	10/31	1,080	5.7	Fall
5/9	730	1.8	Spring	11/7	1,180	5.9	Fall
5/16	650	2.0	Spring	11/14	1,310	6.1	Fall
5/23	580	2.1	Summer	11/21	1,430	6.2	Winter
5/30	500	2.3	Summer	11/28	1,560	6.4	Winter
6/6	450	2.5	Summer	12/5	1,700	6.5	Winter
6/13	400	2.6	Summer	12/12	1,820	6.7	Winter
6/20	360	2.8	Summer	12/19	1,950	6.8	Winter
6/27	310	2.9	Summer	12/26	2,100	7.0	Winter

TABLE 4 Relative Damage Factors by Season of the Year Based on Fatigue Analysis

Thickness (in.)		Seasonal Relative Damage Factors				Thickness (in.)		Seasonal Relative Damage Factors			
Asphalt	Base	Spring	Summer	Fall	Winter	Asphalt	Base	Spring	Summer	Fall	Winter
3	4	.42	.16	.23	.19	4	12	.38	.21	.25	.16
3	7	.42	.16	.23	.19	4	14	.38	.21	.25	.16
3	8	.42	.16	.23	.19	4	15	.38	.21	.25	.16
3	10	.42	.16	.23	.19	4	18	.38	.21	.25	.16
3	11	.42	.16	.23	.19	5	4	.34	.26	.27	.13
3	12	.42	.16	.23	.19	5	7	.34	.26	.27	.13
3	14	.42	.16	.23	.19	5	8	.34	.26	.27	.13
3	15	.42	.16	.23	.19	5	10	.34	.26	.27	.13
3	18	.42	.16	.23	.19	5	11	.34	.26	.27	.13
4	4	.38	.21	.25	.16	5	12	.34	.26	.27	.13
4	7	.38	.21	.25	.16	5	14	.34	.26	.27	.13
4	8	.38	.21	.25	.16	5	15	.34	.26	.27	.13
4	10	.38	.21	.25	.16	5	18	.34	.26	.27	.13
4	11	.38	.21	.25	.16						

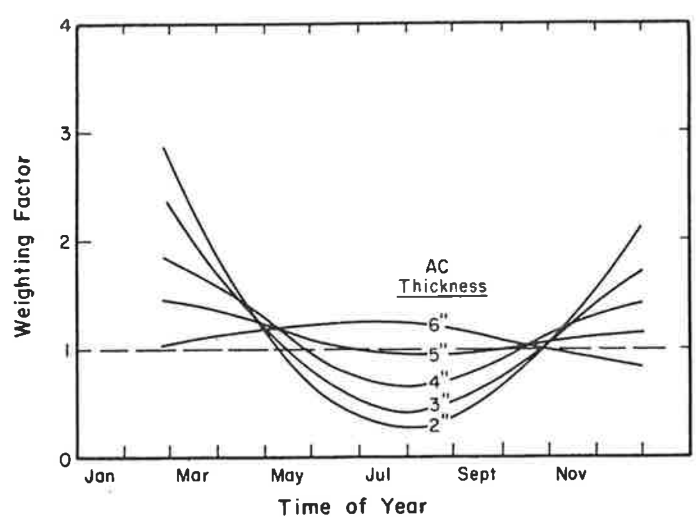

FIGURE 8 Seasonal weighting factors for various thicknesses of AC surfacing.

cording to Figure 8, the shift in critical seasons from spring to summer occurs at about 6 in. of AC.

The damage factor analysis results given in Table 4 also directly correspond to these general seasonal relationships. For each AC thickness (3, 4, and 5 in.), the spring season produced the highest relative damage factor and winter the lowest. The fall damage factor is the second highest for the 3- and 4-in. surfaces. As expected, with increased thickness the spring damage factor decreases and the summer factor increases.

CONCLUSIONS

The analyses reported in this paper demonstrate that the ILLI-PAVE structural model and algorithms provide an adequate and valid representation of the structural behavior of conventional flexible pavements. The structural response-performance relationships explain the observed behavior of the AASHO Road Test pavement sections in a realistic fashion. Seasonal damage factors and weighting factors based on these relationships provide a mechanistic explanation of seasonal effects that is consistent with experience.

The analyses also demonstrate that the ILLI-PAVE analysis algorithms can be used to effectively evaluate NDT data and determine the structural characteristics of existing pavement systems. ILLI-PAVE, therefore, is a powerful tool for pavement design and analysis. It will serve as a sound basis for the development of mechanistic procedures for the design of new flexible pavements and for the selection of rehabilitation strategies for existing flexible pavements.

ACKNOWLEDGMENTS

This paper is based on the results of Project IHR-510, Mechanistic Evaluation of Illinois Flexible Pavement Design Procedures. IHR-510 was sponsored by the Illinois Department of Transportation (Division of Highways) and the U.S. Department of Transportation (Federal Highway Administration).

REFERENCES

1. J.L. Figueroa. Resilient Based Flexible Pavement Design Procedure for Secondary Roads. Ph.D. dissertation. University of Illinois at Urbana-Champaign, 1979.
2. M.S. Hoffman and M.R. Thompson. Mechanistic Interpretation of Nondestructive Pavement Testing Deflections. Civil Engineering Studies, Transportation Engineering Series, No. 32, University of Illinois at Urbana-Champaign, 1981.
3. R.P. Elliott and M.R. Thompson. Mechanistic Design Concepts for Conventional Flexible Pavements. Civil Engineering Studies, Transportation Engineering Series, No. 42, University of Illinois at Urbana-Champaign, 1985.
4. L. Raad and J.L. Figueroa. Load Response of Transportation Support Systems. Journal of the Transportation Engineering Division, ASCE, Vol. 106, No. TE1, Jan. 1980.
5. M.L. Traylor, Jr. Nondestructive Testing of Flexible Pavements. Ph.D. dissertation. University of Illinois at Urbana-Champaign, 1979.
6. M.R. Thompson and Q.L. Robnett. Final Report--Resilient Properties of Subgrade Soils. Civil Engineering Studies, Transportation Engineering Series, No. 14, University of Illinois at Urbana-Champaign, 1976.
7. Research and Development of the Asphalt Institute's Thickness Design Manual (MS-1). 9th ed. Research Report 82-2. The Asphalt Institute, College Park, Md., 1982.
8. The AASHO Road Test, Report 5--Pavement Research. Special Report 61E. HRB, National Research Council, Washington, D.C., 1962.
9. Austin Research Engineers, Inc. Asphalt Concrete Overlays of Flexible Pavements, Vol. 1: Development of New Design Criteria. Report FHWA-RD-75-75. FHWA, U.S. Department of Transportation, 1975.
10. F. Bonnaure, A. Gravois, and J. Udron. A new Method for Predicting the Fatigue Life of Bituminous Mixes. Proc., Association of Asphalt Paving Technologists, 1980.
11. F. Finn, C.L. Saraf, R. Kulkarni, K. Nair, W. Smith, and A. Abdullah. Development of Pavement Structural Subsystems. NCHRP Final Report, Vol. 1, Project 1-10B. TRB, National Research Council, Washington, D.C., 1977.
12. F. Finn, C. Saraf, R. Kulkarni, K. Nair, W. Smith, and A. Abdullah. The Use of Distress Prediction Subsystems for the Design of Pavement Structures. Proc., Fourth International Conference on Structural Design of Asphalt Pavements, University of Michigan, Ann Arbor, 1977.
13. M.R. Thompson. Concepts for Developing a Nondestructive Testing Based Asphalt Concrete Overlay Thickness Design Procedure. Civil Engineering Studies, Transportation Engineering Series, No. 34, University of Illinois at Urbana-Champaign, 1982.
14. M. Gomez-Achecar and M.R. Thompson. Mechanistic Design Concepts for Full-Depth Asphalt Concrete Pavements. Civil Engineering Studies, Transportation Engineering Series, No. 41, University of Illinois at Urbana-Champaign, 1984.

Publication of this paper sponsored by Committee on Flexible Pavements.